

# High-temperature performances of compressed earth blocks stabilized with cementitious binders

Philbert Nshimiyimana<sup>1</sup>[0000-0003-2863-7831], Kader Banaou Djibo<sup>1</sup>, Seick Omar Sore<sup>1,2</sup>,  
Yacouba Coulibaly<sup>1</sup>, Elodie Pru'Homme<sup>3</sup>, Zengfeng Zhao<sup>4</sup>[0000-0002-7059-9085], Adamah  
Messan<sup>1</sup>[0000-0003-1925-1750] and Luc Courard<sup>5</sup>[0000-0001-6573-6631]

<sup>1</sup> Laboratoire Eco-Matériaux et Habitats Durables (LEMHaD), Institut International d'Ingénierie de l'Eau et de l'Environnement (Institut 2iE), 1 Rue de la Science, 01 BP 594 Ouagadougou 01, Burkina Faso

<sup>2</sup> Département Génie Civil de l'Institut Universitaire de Technologie / Laboratoire de Chimie et Energies Renouvelables (LaCER), Unité de Recherche en Physico Chimie et Technologie des Matériaux, Université Nazi BONI, B.P. 1091 Bobo 01, Burkina Faso

<sup>3</sup> MatéIS: MATériaux: Ingénierie et Science, INSA de Lyon, Lyon, France

<sup>4</sup> Department of Structural Engineering, College of Civil Engineering, Tongji University, 1239 Siping Road, Shanghai 200092, China

<sup>5</sup> Urban and Environmental Engineering (UEE), Université de Liège (ULiege), Allée de la Découverte 9, 4000 Liège, Belgium  
`philbert.nshimiyimana@2ie-edu.org`

**Abstract.** The present study assesses the effect of exposure to high temperatures on engineering and durability performances of stabilized compressed earth blocks (CEB). The CEB were produced using clay-rich earthen material stabilized with 8% cement and 10% lime-rich binder. CEB, cured in ambient conditions, were exposed to various temperatures up to 1200 °C for 2 hours. The test results showed that the performances of CEB were maintained or even improved up to a certain temperature. After exposure to 600°C, the dry compressive strength increased from 6.6 to 11.7 MPa ; i.e. 1.8 times; and from 3.2 to 6 MPa; i.e. 1.6 times; respectively for CEB stabilized with cement and lime. It remarkably decreased beyond 600°C. Similar evolutions were observed for the wet compressive strength. The loss of performance after exposure to more than 600 °C was related to the cracks on the surface of the CEB. This was confirmed by the increase of the water absorption capacity of the CEB. After exposure to 1200 °C, the coefficient of capillary absorption exponentially increased 15.6 and 8.2 times respectively for CEB stabilized with cement and lime. Moreover, the coefficient of abrasion resistance was increased from 13.3 to 33.2 cm<sup>2</sup>/g and decreased from 13.3 to 6.2 cm<sup>2</sup>/g up to 600 °C respectively for CEB stabilized with cement and lime. This study shows that the CEB stabilized with cementitious binders can at least maintain their performance up to 600°C.

**Keywords:** compressed earth block, physico -mechanical property, durability, high temperature

## 1 Introduction

There are numerous non-technical advantages and a wide range of architectural possibilities offered by earthen materials in terms of thermal comfort, improved health conditions, and potential energy and economic savings, among others. Many scientific studies have recently been interested in earth as an alternative construction material to

provide sufficient scientific knowledge for the reduction of the share of CO<sub>2</sub> emissions in the building sector. For instance, compressed earth blocks (CEB) are stabilized with mineral cementitious binders such as cement or lime to improve their mechanical and durable performances. Many studies have largely evaluated different properties of stabilized CEB, namely physical, water, mechanical resistances, and durability for applications in ambient conditions [1–7]. However, there have been rare studies that focused on the behavior of stabilized CEB in non-ambient conditions, such as in fire, or other forms of exposure to high-temperatures [6,8–10]. It is therefore important to assess the resistance of such stabilized CEBs when subjected to this type of exposure.

Different water removal processes are involved during the heating of clay materials. There is evaporation accompanied by the loss of free capillary and absorbed water, up to 150°C. Dehydration is accompanied by the loss of bound mechanical and chemical water in between the clay platelets, until around 750 °C. The dehydroxylation is accompanied by the loss of structural water in the form of the hydroxyl groups from the containing minerals such as clay; which can go up to 900-1200 °C. Beyond these temperatures, there is vitrification which can be accompanied by excessive thermal shrinkage [9,11]. These phenomena may occur simultaneously and would rather depend on the existing compounds in the clay materials, the environment, and the rate of heating. Rapid heating can cause a steam atmosphere to persist outside and inside the bricks, causing restrictive circumstances which can result in discoloration [6].

It is therefore important to assess the performances of CEB when they are exposed to undesired high temperatures during their service life such as in scenario of fire or for application at high temperatures. In fact, there have been some interests in using CEB for envelope of incinerators or furnaces for various applications (**Fig. 1**). Some preliminary studies have attempted to assess the behaviors of different composition of earth-based materials exposed to high temperatures with various interests such as the evaluation of the thermal instability of unstabilized rammed earth, the effect of water content and stabilization, effect on the compressive and abrasion resistance [6,8–10,12].

The present study aims to assess the effect of high temperature on engineering properties and some durability indicators of CEB stabilized with cementitious mineral binders. It specifically evaluates the physico-mechanical and water resistances of the stabilized CEB before and after exposure to high temperature.



**Fig. 1.** Illustration view of incinerators at a) SONABEL and b) ISIG in Bobo Dioulasso, Burkina Faso

## 2 Materials and Methods

### 2.1 Materials

Clayey earthen materials commonly called laterite was used as the main matrix of CEB. The cementitious binders for the stabilization of CEB consist of the Portland cement (CEM), and lime-rich calcium carbide residue (CCR). The lateritic earth was collected from the locality of Kamboinsé located 15 km North of Ouagadougou. This laterite had been previously characterized for its suitability to produce stabilized CEB. The physicochemical and mineralogical characterization showed that this material behaves as a clay-silt of medium to high plasticity and contains up to 75 % of kaolinite clay and quartz minerals. It was suitable to produce stabilized CEB [13]. The cement is CEMII/AP/42.5 N, produced by Diamond Cement factory around Ouagadougou. The lime-rich CCR is an industrial by-product from the production of acetylene gas by the local company BIG (Burkina Industrial Gas). The CCR contains up to 50% of  $\text{Ca(OH)}_2$  and various forms of  $\text{Ca(CO)}_3$ . It was also previously used to stabilize CEB after grinding and sieving down to a particle size of 400  $\mu\text{m}$  [2].

### 2.2 Production and Curing of CEB

The CEB were produced from the two types of mix design: stabilization with 8% cement (CEM-CEB) and stabilization with 10% CCR (CCR-CEB), as recommended from the previous study [13] [2]. Firstly, the dry mixture of earth and binder was homogenized; and then humidified with water at the respective optimum water content of each mix [2]. The wet mixtures were poured into a  $29.5 \times 14 \times 9.5 \text{ cm}^3$  prismatic mold of a TERSTARAM manual press and compressed to produce CEB.

The CEB were carefully covered in polymeric bags and stored for curing at the ambient temperature of the laboratory  $30 \pm 5^\circ\text{C}$ , at the production humidity. The curing in polymeric bags allows the CEB to retain their humidity for the hydration and/or pozzolanic reaction take place properly for the stabilization with cement or lime, respectively. The curing period was 28 days for the CEM-CEB and 45 days for the CCR-CEB, according to previous study [14]. After the curing, the CEB were slowly dried to constant mass in an oven at  $60^\circ\text{C}$  and exposed to high temperature.

### 2.3 Exposure to High Temperatures

The CEB were placed in an LH 30/14 furnace and exposed to various high temperatures at a heating rate of  $5^\circ\text{C}/\text{min}$  and soaking time of 2 hours. The CEB were heated to the maximum temperatures of  $300^\circ\text{C}$ ,  $600^\circ\text{C}$ ,  $900^\circ\text{C}$ ,  $1200^\circ\text{C}$ . **Fig. 2** presents the three stages heating profile: the heating phase at  $5^\circ\text{C}/\text{min}$ , the soaking phase of 2 hour, and finally the cooling phase in the furnace. After exposure to high temperatures, the CEB were inspected for any physical changes on their surface.

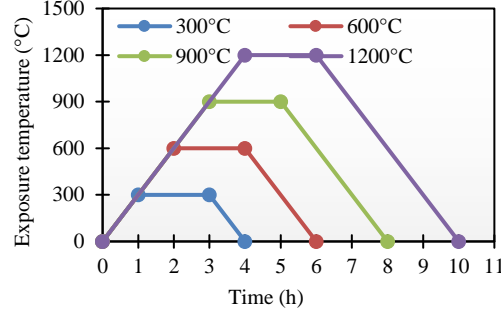


**Fig. 2.** Heating profile of CEB over the time

## 2.4 Characterization of CEB

The physico-mechanical and durability properties of CEB were tested before and after exposure to high temperatures. Capillary water absorption was determined according to PR XP P 13-901 [15]. The dry samples were partially immersed at a constant water height of 0.5 cm and weighed over a period of 24 hours. The variation of the mass ( $M_t - M_0$  in g) of the specimen due to capillary absorption through the surface ( $S$  in  $\text{cm}^2$ ) over time allowed to determine the coefficient of capillary absorption ( $C_a$  in  $\text{g}/\text{cm}^2$ ) using equation 1. The bulk density, water accessible porosity and total water absorption were characterized through the hydrostatic weighing test, following NF P18-459 [16]. It consists of weighing the specimen in dry and saturated conditions; the dry mass ( $M_{\text{dry}}$  in kg), the saturated mass weighed in air ( $M_{\text{sat.air}}$  in kg), and the saturated mass weighed in water ( $M_{\text{sat.water}}$  in kg). Knowing the density of water ( $\rho_{\text{water}}$  in  $\text{kg}/\text{m}^3$ ) allows to determine the water accessible porosity (WAP in %), the bulk density ( $\rho_b$  in  $\text{kg}/\text{m}^3$ ) and the total water absorption (TWA in %) of CEB respectively in equations 2, 3, and 4.

$$C_a = \frac{M_t - M_0}{S} \quad (1)$$

$$\text{TWA} = \frac{M_{\text{sat.air}} - M_{\text{dry}}}{M_{\text{dry}}} \times 100 \quad (2)$$

$$\text{WAP} = \frac{M_{\text{sat.air}} - M_{\text{dry}}}{M_{\text{sat.air}} - M_{\text{sat.water}}} \times 100 \quad (4)$$

$$\rho_b = \frac{M_{\text{dry}} \times \rho_{\text{water}}}{M_{\text{sat.air}} - M_{\text{sat.water}}} \quad (5)$$

The compressive resistance was determined on dry and wet CEB, after two hours immersion in water, according to PR XP P13-091 [15], using a hydraulic press (ETI-PROETI) which has a capacity a capacity of 300 kN. The test was carried out at loading speed of 0.02 mm/s until the failure of the specimens. The maximum load to failure ( $F_{\text{max}}$  in N) and the cross-section area of the specimens ( $S$  in  $\text{cm}^2$ ) allow to determine the values of the compressive resistances ( $R_c$  in MPa), in equation 5. The abrasion resistance was determined on dry and wet CEB, according to PR XP P13-091

[15], using a steel wire brush loaded with a mass of 3 Kg. The specimen was brushed by 60 rounds on a surface ( $S$  in  $\text{cm}^2$ ) and the mass of the specimen ( $M_1$  in g), after the test, was compared to the mass of the specimen ( $M_0$  in g), before the test. The coefficient of resistance to abrasion ( $C_b$  in  $\text{cm}^2/\text{g}$ ) was calculated using equation 6.





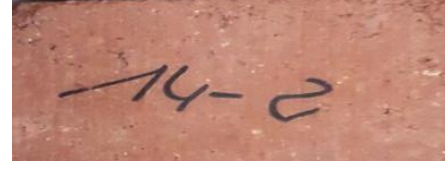

$$R_c = 10 \times \frac{F_{\max}}{S} \quad (5)$$

$$C_b = \frac{S}{M_0 - M_1} \quad (6)$$

### 3 Results and Discussion

#### 3.1 Effect on visual aspects of CEB

The CEB stabilized with cementitious binders underwent color changes throughout the exposure to high temperature. **Fig. 3** shows that the color of CEB changed from pale brown to dark brown/grey, respectively for CEM-CEB and CCR-CEB. These changes can be related to several thermochemical reactions, including the dehydroxylation of clay mineral and oxidation of ferrous minerals in the brick, which occur when the temperature reaches 600-1200 °C [11]. The surface of the CEB exposed to 1200 °C shows the visible cracks which can be related to the thermal shock. These cracks would be linked to unconstrained volume expansion, which initiates crack propagation. The color change to dark grey of CCR-CEB can be related to the decomposition of  $\text{Ca}(\text{CO}_3)_3$ , initially from the CCR or formed by the carbonation of  $\text{Ca}(\text{OH})_2$ , which shows very remarkable cracks and a burn color [11].

Temp	CEB stablized with CEM	CEB stablized with CCR
1200 °C		
600 °C		
Tamb		

**Fig. 3.** Effect on appearance of CEB stabilized with CEM (left) and CCR (right)

### 3.2 Effect on Bulk density and water accessible porosity

**Fig. 4** presents the evolution of bulk density and water-accessible porosity of stabilized CEB after exposure to high temperature, relatively to the bulk density and porosity at ambient temperature. It shows that the apparent density decreases (0.9 times) inversely with the increase of the porosity (1.2 times), with the increases of the exposure temperature. This can be related to the loss of the mechanical water, the production water, which remained after the initial drying at 60°C and subsequently the chemical water [11]. The CEM-CEB exposed to 1200 °C reached the highest porosity (32 %) and the lowest density of 1661 kg/m<sup>3</sup>; while they had the porosity of 26% and the density of 1861 kg/m<sup>3</sup> at room temperature. The CCR-CEB exposed to 1200 °C reached the porosity of 38 % and the density of 1641 kg/m<sup>3</sup> respectively from 33% and 1749 kg/m<sup>3</sup> at ambient temperature (**Fig. 4**).

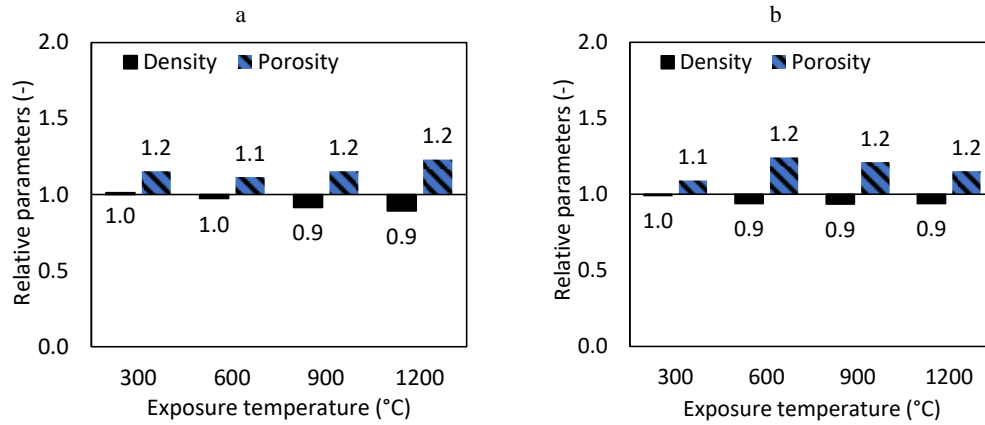


**Fig. 4.** Evolution of bulk density and water accessible porosity with the exposure temperature of CEB stabilized with a) CEM and b) CCR

**Table 1.** Evolution of the coefficient of absorption of CEB stabilized with CEM and CCR

CEB	Temp (°C)	$\rho_b$ (kg/m <sup>3</sup> )	WAP (%)	S (g/cm <sup>2</sup> .min <sup>0.5</sup> )	$C_{b10min}$ (g/cm <sup>2</sup> .min <sup>0.5</sup> .)	Class [15]	TWA (%)
CEM	Tam	1861	26	0.08	7	Very slightly capillary	9.0
	300	1885	30	0.1	9	Very slightly capillary	11.7
	600	1812	29	0.23	15	Very slightly capillary	17.1
	900	1704	30	-	57	-	18.6
	1200	1661	32	-	104	-	20.5
CCR	Tam	1749	33	0.13	13	Very slightly capillary	18.3
	300	1735	36	0.14	11	Very slightly capillary	20.4
	600	1642	41	0.34	19	Very slightly capillary	24.4
	900	1635	40	-	60	-	23.8
	1200	1641	38	-	103	-	22.6

$\rho_b$  = Bulk density, WAP = Water accessible porosity,  $C_{b10min}$  = Coefficient of capillary absorption initially in macropore in the first 10 minutes; S = sorptivity coefficient of capillary absorption in capillary pores, TWA = Total water absorption

At ambient temperature, the hydration products formed from the cement and lime such as the calcium silicates (CSH) bind the particles of the matrix and thus creating

the densification of the CEB [3]. At higher temperature, the dehydration and dehydroxylation phenomena created supplementary porosity, eventually accompanied by the formation of cracks which created more porosity and therefore lesser mass weigh [9].

### 3.3 Effect on Water Absorption

The evolution of water absorption over the exposure to high temperature was assessed on the rate of capillary absorption and the capacity of absorption by total immersion. **Fig. 5** shows the rate of capillary absorption (sorptionity) of CEB in capillary pore, between 1 hour and 24 hours or the saturation. It shows that the rate increases with the exposure temperature, and more drastically beyond 600°C, where the absorption reaches the saturation before the first hours. This rate of capillary absorption is higher for materials which have larger diameter of capillary pore [17]. In fact, the first absorption (the first rate in the first hour) takes place in the macropores, and the late in the capillary pores [1]. This confirms that the exposure of CEB to higher temperature (>600 °C) creates more macropore than capillary pores related to the formation of surface and possibly internal cracks. The sorptivity increased from 0.08 to 0.23 g/cm<sup>2</sup>.min<sup>0.5</sup> and 0.13 to 0.34 g/cm<sup>2</sup>.min<sup>0.5</sup> respectively for CEM-CEB and CCR-CEB (**Fig. 5**). This suggests a relative increase of the diameter of capillary pores during the drying phase in the first 600 °C, followed by the crack degradations and formation of macropores beyond the 600 °C.

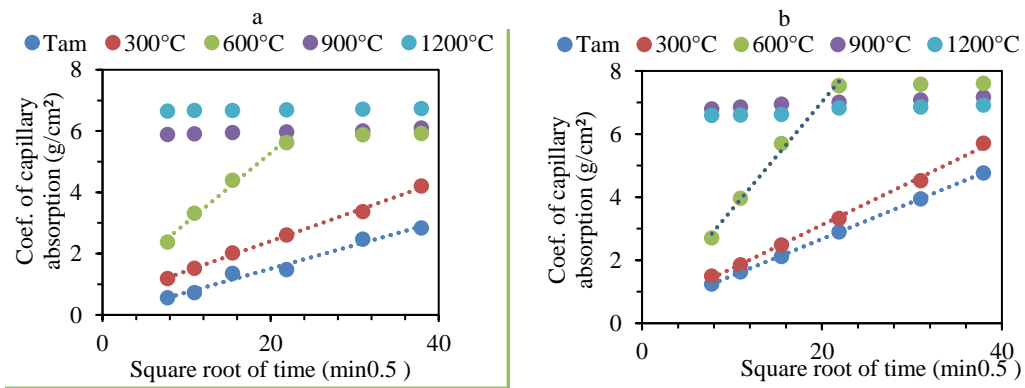


**Fig. 5.** Evolution of capillary absorption rate of stabilized with : a) CEM, b) and CCR

The coefficient of capillary absorption initially in macropore was also evaluated in the first 10 minutes ( $C_{b10min}$ ). The  $C_{b10min}$  effectively increased with the exposure temperature up to 15.6 times and 8.2 times respectively for CEM-CEB and CCR-CEB (**Table 1**); which were from 7 to 104 g/cm<sup>2</sup>.min<sup>0.5</sup>.% and from 13 to 103 g/cm<sup>2</sup>.min<sup>0.5</sup>.% (**Table 1**). These CEB can still be labelled as very slightly capillary up to 600°C, as their  $C_{b10min}$  was still lower than 20 g/cm<sup>2</sup>.min<sup>0.5</sup>.%, beyond which the  $C_{b10min}$  was higher than the up limit of 40 g/cm<sup>2</sup>.min<sup>0.5</sup>.% slightly capillary CEB. In fact, a quasi-exponential increase of the  $C_{b10min}$  was observed beyond 600 °C; which shows a drastic increase in the macropores related back to the formation of the cracks (3.1). This can generally be

explained by the evaporation and dehydration phase which created the porosity and made the CEB sensitive to water absorption [18]. From 900 °C, the pores became larger and eventually continuous/ connected due to the cracks formation possibly associated with the transformation of minerals and/or thermal shock. This had negative effect of the absorption coefficient, precisely the  $Cb_{10min}$ .

The water absorption capacity by total immersion for 24 hours (TWA) evolved like capillary absorption. **Fig. 6** shows that the increase of the exposure temperature, increased the TWA up to 2.3 times and 1.3 times respectively for CEM-CEB and CCR-CEB. **Table 1** shows that the TWA reached 17.1 % and 24.4 % after exposure to 600 °C, from 9 % and 18.3 % at room temperature respectively for CEM-CEB and CCR-CEB. Beyond the 600 °C, the TWA kept increasing for CEM-CEB and slightly decreased for CCR-CEB. This suggests that the crack observed on the CEB beyond the 600 °C were deeper and more connected in CEM-CEB than in CCR-CEB. It made the TWA reaches more than 20 % recommended for CEB useful in contact with water [19].

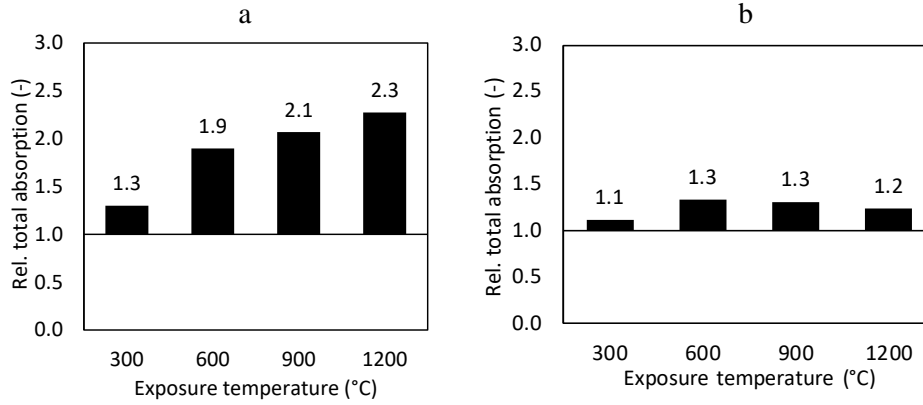


**Fig. 6.** Evolution of total water absorption by total of CEB stabilized with: CEM and b) CCR

### 3.4 Effect on Compressive resistance

**Fig. 7** presents the evolution of the dry and wet compressive resistance of stabilized CEB with exposure temperatures. Increasing the exposure temperature up to 600°C increased the dry resistance up to 1.8 times and 1.6 times and the wet resistance up to 1.7 times and 1.7 times respectively for CEM-CEB and CCR-CEB. The increase of the dry compressive resistance was in the ranges of 6.6 to 11.7 MPa and 3.2 to 6 MPa for CEM-CEB and CCR-CEB, respectively. This increase can be related to the dry-hardening effect with exposure up to 600 °C, which increased more the compressive resistance in the dry conditions ( $R_{cd}$ ) than in wet condition ( $R_{cw}$ ). In fact, the ratios  $R_{cw}/R_{cd}$  decreased from 0.71 to 0.67 for CEM-CEB and slightly increased from 0.65 to 0.69 for CCR-CEB (**Table 2**). This is due to the increase of the water accessible porosity and the sensibility to water. Although, both the dry and wet resistance decreased beyond 600 °C (**Table 2**), the ratios  $R_{cw}/R_{cd}$  increased to 1.08 for CEM-CEB and 0.91 for CCR-CEB at 1200 °C (**Table 2**). This can be related to the firing effect



which maintained the same stability of the CEB in dry and wet conditions, even though the porosity and cracks kept increasing.

The evolution of the resistance is comparable to the 58 % increase (4.2 to 6.6 MPa) previously reported for CEB stabilized with 8% cement and heated at 600°C [6]. Bakam et al [8] also reported a strength of 1.2 MPa and 2.4 MPa for CEB stabilized with 2% cement respectively exposed to 200°C and 800°C. **Table 2** classifies CEB before and after exposure to high temperature, according to the PR XP P 13-901 [15]. Moreover, the coefficient of structural efficiency (CSE), ratio  $R_{cd}/\rho_b$ , increased 1.8 times for CEM-CEB and 1.7 times for CCR-CEB until 600 °C, then decreased. This confirms that the structural stability of CEB was maintained until 600 °C. Therefore, the structural class of CEB varied from CEB60, CEB which can withstand a stress of 6 MPa, down to CEB20 that can withstand 2 MPa in dry conditions. It is noteworthy that CEB60 can be used in load-bearing in wall masonry [20].

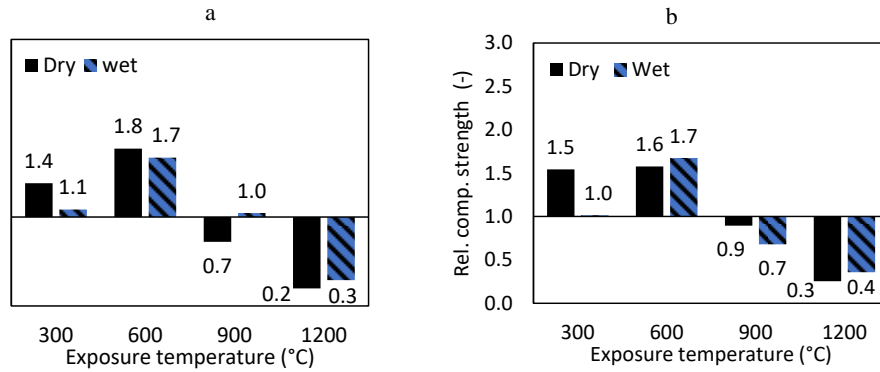


**Fig. 7.** Evolution of resistance to compression with the exposure temperature of CEB stabilized with a) CEM and b) CCR

**Table 2.** Classification of CEB based on the compressive and abrasive resistance

CEB	Temp (°C)	R <sub>cd</sub> (MPa)	R <sub>cw</sub> (MPa)	R <sub>cw</sub> /R <sub>cd</sub> (-)	Class [15]	CSE (J/kg)	Ca (cm <sup>2</sup> /g)	Class [15]
CEM	Tam	6.6	4.7	0.71	CEB60	3546	23	CEB60
	300	9.1	5.1	0.56	CEB60	4838	33	CEB60
	600	11.7	7.9	0.67	CEB60	6446	33	CEB60
	900	4.8	4.9	1.03	CEB40	2795	27	CEB60
	1200	1.3	1.4	1.05	CEB10	779	5	CEB20
CCR	Tam	3.2	2.1	0.65	CEB20	1836	13	CEB60
	300	5	2.1	0.43	CEB40	2856	8	CEB60
	600	5.1	3.5	0.69	CEB60	3087	6	CEB40
	900	2.9	1.4	0.49	CEB20	1759	5	CEB20
	1200	0.8	0.8	0.91	-	500	4	CEB20

R<sub>cd</sub>/w = Compressive resistance in dry/wet conditions, CSE = Coefficient of structural efficiency

### 3.5 Effect on Abrasion Resistance

The coefficient of abrasion resistance ( $C_b$ ) evolved for CEM-CEB differently to CCR-CEM. The  $C_b$  was stable until 600 °C for CEM-CEB and decreased down to 0.2 times; contrary to the CCR-CEB which decreased immediately and continuous down to 0.3 times (**Table 2**). This suggests that the CCR-CEB suffered more surface and superficial degradations from the beginning of exposure to high temperature than the CEM-CEB which rather suffered deeper degradation and at higher temperature (1200 °C). **Table 2** shows that all the CEB maintained at least the class of CEB40, with at least the  $C_b$  of 5 cm<sup>2</sup>/g until 600 °C [7] .

## 4 Conclusion

The overall objective of this study was to assess the performance of CEB stabilized with cementitious binders at high temperature. In this study, the interest was to determine the residual engineering properties and durability indicators of CEB. The results of the various tests show that increasing the exposure temperature up to 600°C generally improves the main properties of CEB, followed by the loss some performances up until 1200 °C tested in the present study.

The CEB maintained the physical (surface stability) until 600 °C and underwent significant crack degradations beyond. These cracks drastically increased the (water accessible) porosity and water absorption (rate) due to the drying and burning effects. Similarly, the structural stability was improved until 600 °C, and decreased. However, the burning effect improved the water sensitivity of CEB, as their compressive resistance in wet condition was almost as similar as the resistance in dry condition. More specifically, exposure to high temperatures increased the compressive resistance from 6.6 to 11.7 MPa for CEM-CEB and from 3.2 to 6 MPa for CCR-CEB in dry condition, allowing to reach a structural class of CEB60 for load-bearing at lower than 600°C. Although the coefficient of surface abrasion resistance continuously decreased, it remained higher than 7 cm<sup>2</sup>/g required for CEB60, except for CCR-CEB, until 600 °C. Furthermore, the increase of the coefficient of capillary absorption initially in macropores ( $C_{b10min} < 20 \text{ g/cm}^2 \cdot \text{min}^{0.5} \cdot \%$ ) and the sorptivity in the capillary pores ( $S < 0.34 \text{ g/cm}^2 \cdot \text{min}^{ss}$ ) was relatively limited until 600 °C to classified the CEB as weakly capillary.

This study allows to conclude that the performances of CEB stabilized with cementitious binders are relatively stable up until exposure to 600 °C. Beyond this temperature, the precautions need to be taken in terms of structural stability in both dry and wet conditions to fulfill the designed application.

## References

1. Nshimiyimana P, Messan A, Courard L. Hydric and durability performances of compressed earth blocks stabilized with industrial and agro by-product binders : calcium carbide residue and rice husk ash. *Journal of Materials in Civil Engineering*. 2021;33:04021121.

2. Nshimiyimana P, Messan A, Courard L. Physico-mechanical and hygro-thermal properties of compressed Earth Blocks stabilized with industrial and Agro By products Binders. *Matériaux*. 2020;13:37–69.
3. Nshimiyimana P, Messan A, Courard L. Physico-Mechanical and Hygro-Thermal Properties of Compressed Earth Blocks Stabilized with Industrial and Agro By-Product Binders. *Materials*. 2020;13:3769.
4. Tarmangue D, Sore SO, Nshimiyimana P, Messan A, Courard L. Comparative Study of the Reactivity of Clay Earth Materials for the Production of Compressed Earth Blocks in Ambient Conditions: Effect on Their Physico- Mechanical Performances. *Journal of Mineral and Materials characterization and engineering [Internet]*. 2021;10:40–56.
5. Kiki G, Nshimiyimana P, Kouchadé C, Messan A, Houngan A, André P. Physico-mechanical and durability performances of compressed earth blocks incorporating quackgrass straw: An alternative to fired clay. *Constr Build Mater*. 2023;403:133064.
6. Nshimiyimana P, Hema C, Sore SO, Zoungrana O, Messan A, Courard L. Durability performances of compressed earth blocks exposed to wetting-drying cycles and high temperature. *WIT Transactions on The Built Environment*. 2022;210:141–9.
7. Nshimiyimana P, Sore SO, Hema C, Zoungrana O, Messan A, Courard L. A discussion of “Optimisation of Compressed Earth Blocks (CEBs) using natural origin materials: A systematic literature review.” *Constr Build Mater*. 2022;309:126887.
8. Bakam VA, Mbishida MA, Danjuma T, Zingfat MJ, Hamidu LAJ, Pyendang ZS. Effect of Firing Temperature on Abrasive and Compressive Strengths of an Interlocking Compressed Stabilized Earth Block (CSEB). *International Journal of Recent Engineering Science*. 2020;7:44–6.
9. Beckett C, Kazamias K, Law A. Investigations into the high temperature behaviour of unstabilised rammed earth. *Sustainable Construction Materials and Technologies*. 2019;3.
10. Abdallah R, Perlot C, Carré H, Borderie C La, Ghoche H El. Fire Behavior of Raw Earth Bricks : Influence of Water Content and Cement Stabilization. 2022;1:792–800.
11. Akinshipe O, Kornelius G. Chemical and Thermodynamic Processes in Clay Brick Firing Technologies and Associated Atmospheric Emissions Metrics-A Review. *Journal of Pollution Effects & Control*. 2017;05.
12. Lawaneb A, Minane JR, Vinai R, Pantet A. Mechanical and physical properties of stabilised compressed coal bottom ash blocks with inclusion of lateritic soils in Niger. *Journal of scientific African*. 2019;0–33.
13. Nshimiyimana P, Fagel N, Messan A, Wetshondo DO, Courard L. Physico-chemical and mineralogical characterization of clay materials suitable for production of stabilized compressed earth blocks. *Constr Build Mater*. 2020;241.
14. Nshimiyimana P, Messan A, Zhao Z, Courard L. Chemico-microstructural changes in earthen building materials containing calcium carbide residue and rice husk ash. *Constr Build Mater [Internet]*. 2019;216C:622–31.
15. PR XP P13-901. Blocs de terre comprimée pour murs et cloisons - Définitions - Spécifications - Méthodes d'essai - Conditions de réception. AFNor, editor. Saint-Denis La Plaine Cedex; 2017.
16. NF P 18-459. Essai pour béton durci - Essai de porosité et de masse volumique. AFNor, editor. Saint-Denis La Plaine Cedex; 2010.
17. Longhi MA, Rodríguez ED, Walkley B, Eckhard D, Zhang Z, Provis JL, et al. Metakaolin-based geopolymers: Efflorescence and its effect on microstructure and mechanical properties. *Ceram Int*. 2021
18. Yong-sing N, Yun-ming L, Cheng-yong H, Mustafa M, Bakri A, Pakawanit P, et al. Thin fly ash / ladle furanace slag geopolymer : Effect of elevated temperature exposure on flexural properties and morphological characteristics. *Ceram Int*. 2022
19. Bogas JA, Silva M, Gomes M da G. Unstabilized and stabilized compressed earth blocks with partial incorporation of recycled aggregates of recycled aggregates. *international journal of architectural Heritage*. 2018;3058:1–16.
20. CDI&CRATerre. Compressed Earth Blocks- Standards: Guide technologies series N° 11. Boubekeur S, Houben H, Doat P, D’Ornano S, Douline A, Garnier Ph, et al., editors. Brussels; 1998.